

Chapter 2

Heat Capacity and Entropy Functions in Strong and Fragile Glass-Formers, Relative to Those of Disordering Crystalline Materials

C. Austen Angell

2.1 Introduction

The glassy state problem is often separated into two major components [1, 2]. One of these concerns the reasons that glasses form in the first place, and deals with the circumstance that glasses are usually metastable with respect to crystals so that crystallization must be avoided. The second deals with the question of how liquids behave when crystals do not form, and it is with this component that we are concerned in this chapter. Here the central phenomenon with which we must deal, in seeking to understand vitrification, is the heat capacity function and the change in that function that accompanies the freezing in of the disordered state. This phenomenon is illustrated in Fig. 2.1 for a typical molecular liquid, 2-pentene vitrified by both liquid cooling and by vapor deposition [3].

The fairly abrupt change in heat capacity that is observed as the system falls out of equilibrium (essentially because the systems' molecular motions have become too sluggish to follow the cooling) irrespective of whether the substance under study is a liquid, a plastic crystal, or a disordered superlattice. It is the phenomenon that many would consider to be the most characteristic feature of glassformers and vitrification . . . and yet, for the archetypal glassformer SiO_2 in its purest anhydrous state, and for glassy water –the most abundant form of water in the universe – this change in heat capacity on structural arrest during cooling is barely detectable [4]. It is not surprising that the vitrification of liquids is found to be the source of much confusion.

It is clear to any reader of the recent literature on glassforming liquids (now “glassformers”) that investigators in the field have given most of their attention to the spectacular manner in which the majority of glassformers change their viscosity

C.A. Angell (✉)

Department of Chemistry and Biochemistry, Arizona State University,
Tempe, AZ 85287-1604, USA
e-mail: austenangell@gmail.com

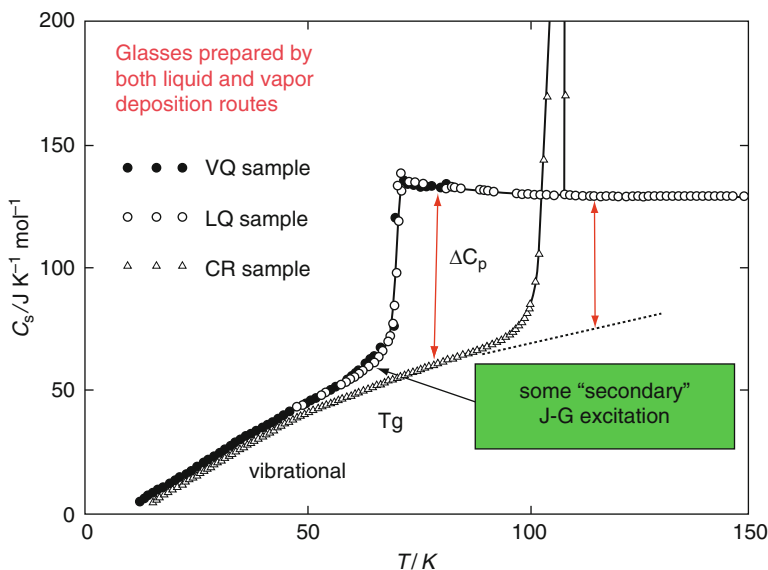


Fig. 2.1 Heat capacity of 1-pentene prepared by both liquid cooling and by vapor deposition. The excess heat capacity is indicated by double arrows and is seen to increase markedly with decreasing temperature (From Takeda et al. Ref. [3], by permission)

(or relaxation times) on approach to the glass transition. In the most interesting cases now known as “fragile” liquids [5, 6], the temperature dependence of viscosity departs dramatically from the Arrhenius equation typical of most rate processes in condensed matter, accelerating as the glass transition is approached to such an extent that a temperature change of 3 K can induce an order of magnitude change in viscosity. The behavior is not as dramatic as the power law divergences observed in critical phenomena, but in some cases this behavior is approached. Indeed, as we will discuss further below, this is probably not an accident.

Most theories for the viscosity (or, more generally, for the relaxation time) connect viscosity temperature dependence to the temperature dependence of one or other thermodynamic property. In the 1959 free volume model of Cohen and Turnbull [7], the thermodynamic property was the unoccupied volume (integral of an expansivity component), in Adam-Gibbs theory [8] it was the configurational part of the entropy (integral of a heat capacity component), while the more recent “shoving model” of Dyre and colleagues [9] use the temperature dependence of a modulus, the “infinite frequency” shear modulus, to explain the super-Arrhenius behavior. So a proper appreciation of the thermodynamic properties of the glassformer would seem to be a prerequisite of a detailed understanding of the transport behavior.

Here we will consider the highly variable forms that the heat capacities of glass-forming liquids can take, and will then show that, in spite of this great variation, the integrals of the heat capacities, the entropies, $S = \int C_p dT$ – and particularly its excess over the entropy due to vibrations – fall into a pattern that mimics the well-known pattern made by the viscosities of glassformers when plotted in T_g -scaled Arrhenius

form (the “strong/fragile” liquid pattern). While the origin of the “strong/fragile” pattern for viscosities (and relaxation times) remains more or less mysterious, the pattern for the entropies can be simply reproduced using a two-parameter model of configurational excitations [10], as will be demonstrated. Finally, we will interpret the “strong liquid” extreme of this pattern in a provocative way by showing the similarity that the heat capacity function for these liquids bears to a well-known heat capacity form for disordering excitations in solids, the lambda transition.

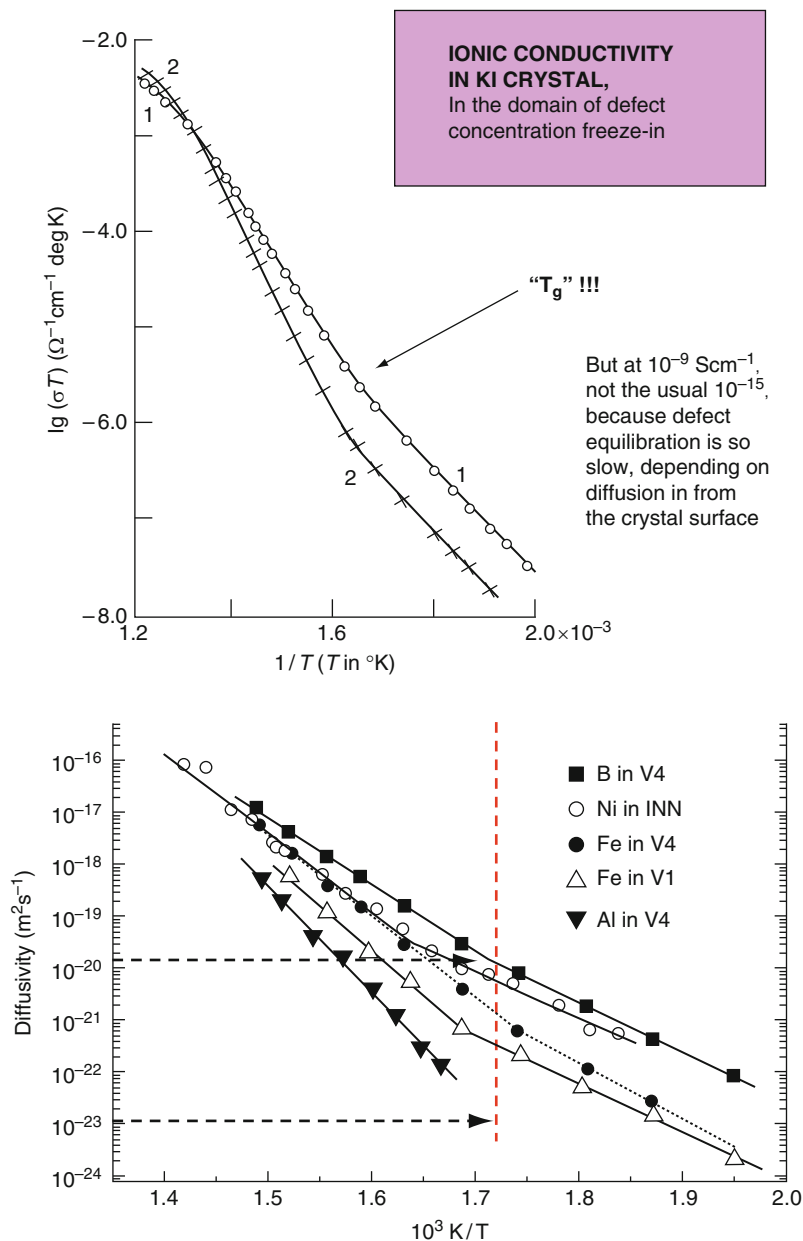
The entropy variations can be accounted for quite pleasingly with the help of a simple two-state excitations model [11], provided that apparently pathological systems like water and silicon, which are extremely poor glassformers by liquid routes, and the liquids classified as “strong” on the basis of their viscosity data, are excluded. Even the latter follow the expectations of two-state excitations when only very high temperature data, obtained by computer simulation, are considered [12]. This encourages consideration of the possibility that the much more challenging pattern offered by the heat capacities themselves might have a systematic explanation. As an aid to understanding this problem we include consideration of the relatively well-understood cases of disordering solids, the order–disorder transitions or lambda transitions.

Before launching into a review of the heat capacity functions, their integrals and their patterns of behavior, let us give some brief consideration to non-glassy systems in which structural arrest of ordering processes is commonly observed. Since the archetypal glassformer, silica, has barely any thermal signature of the glass transition, we cannot make a large jump in heat capacity on structural arrest a criterion for inclusion in the discussion. Thus we start with the simplest and most familiar case, the freezing in of a defect population during the cooling of a simple crystal, for instance potassium iodide.

We do not know of any heat capacity studies of this trapping of the configurational state of the system, but its generic relation to the glass transition phenomenology can be judged from a comparison of a quantity which, like the viscosity of silica, is exponentially sensitive to the freezing of the excitation population. This is the ionic conductivity, which is shown in Arrhenius form in Fig. 2.2, in the form preferred by many in the ionics field because it is suggested by theoretical treatments, viz., $\log(\sigma T)$ vs $1/T$ where σ is the specific conductivity. Comparison is made with the variation of the diffusivities of different elemental components of various metallic glassformers through their T_g s [13].

Notwithstanding the similarity of Fig. 2.2a, b, the metallic glassformers of Figure 2b have quite marked heat capacity jumps at their T_g s. At higher temperatures it becomes clear, also, that their diffusivities follow a super-Arrhenius path in temperature, though in the temperature domain immediately above T_g they are usually following the Arrhenius law with higher activation energies than below T_g .

Passing to systems that begin to resemble glassformers a little more closely, we show the relaxation times for some ionic crystal rotator phases, in which the rotation of a structural element causes little distortion of the crystal lattice. A series of these were studied by Fujimori and Oguni [14], and their relaxation time behavior is shown in Fig. 2.3a. In this case the thermal consequences of the structural arrest at the “glass



This figure will be printed in b/w

Fig. 2.2 (a) Temperature dependence of ionic conductivity in single crystal of potassium iodide in the temperature range where the defect population freezes in for this crystal dimension. (b) Temperature dependence of metallic diffusivity of atomic components through T_g in different metallic glasses (From Faupel et al. Ref. [13], by permission)

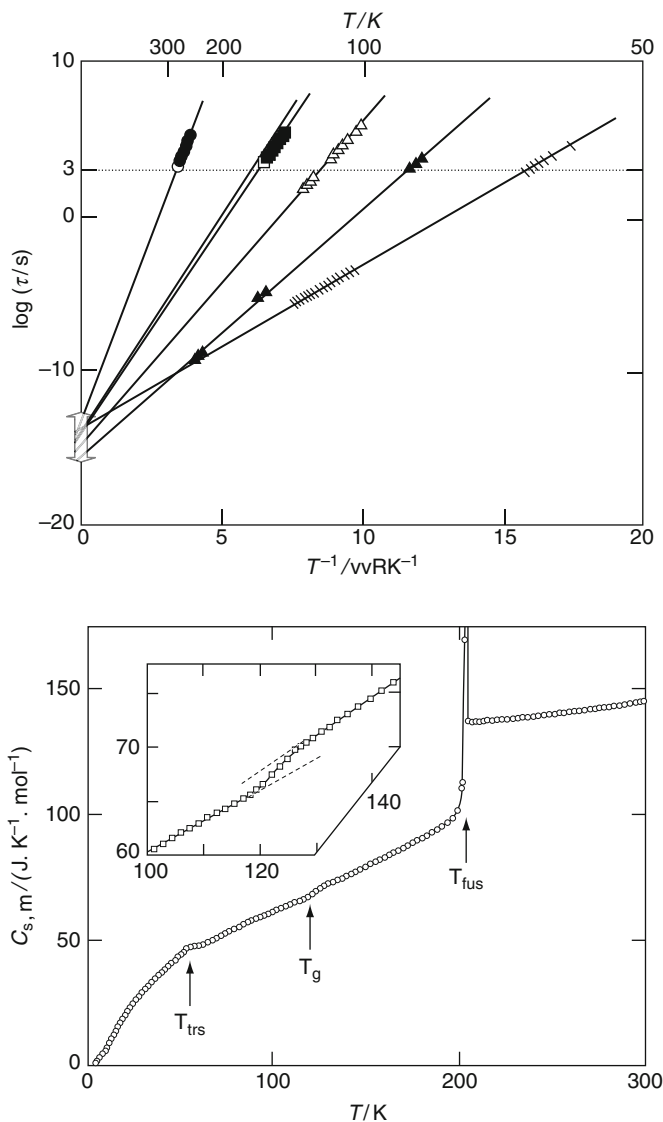


Fig. 2.3 (a) Arrhenius plots of the dielectric (higher T points) and calorimetric relaxation times (lower T points) for several rotator phases (in order from *left*) H_3BO_3 , D_3BO_3 (identical curve with H_3BO_3 one), $\text{SnCl}_2 \cdot 2\text{H}_2\text{O}$, $\text{SnCl}_2 \cdot 2\text{D}_2\text{O}$, $\text{C}_4\text{H}_3\text{BrS}$, Cm, TiNO_2 (From Fujimori and Oguni Ref. [14]). (b) The weak jump in heat capacity that accompanies the glass transition in $\text{C}_4\text{H}_3\text{BrS}$, typical of the systems with the relaxation time behavior seen in Fig. 2.3a (From Fujimori and Oguni Ref. [15], by permission)

temperature” (which was characterized by a relaxation time of 1,000 s in this case) were determined, and the results are shown in Fig. 2.3b for one case, bromothiophene [15]. Clearly the glass transition is a very weak phenomenon in this case (and others

like it [16]), and accordingly the relaxation times are in good accord with the Arrhenius law.

Other cases of disordering processes with relaxation time behavior that follows the Arrhenius law, also have very weak thermal signatures of structural arrest, but an overall more interesting heat capacity behavior. One of the more relevant is the large quasi-spherical molecule, C_{60} , the packing of which has a dipolar excitation and so can be studied by dielectric relaxation. The relaxation process also follows the Arrhenius law, as might be expected from the tiny change of heat capacity at its “glass transition”. The heat capacity in this case is shown in Fig. 2.4.

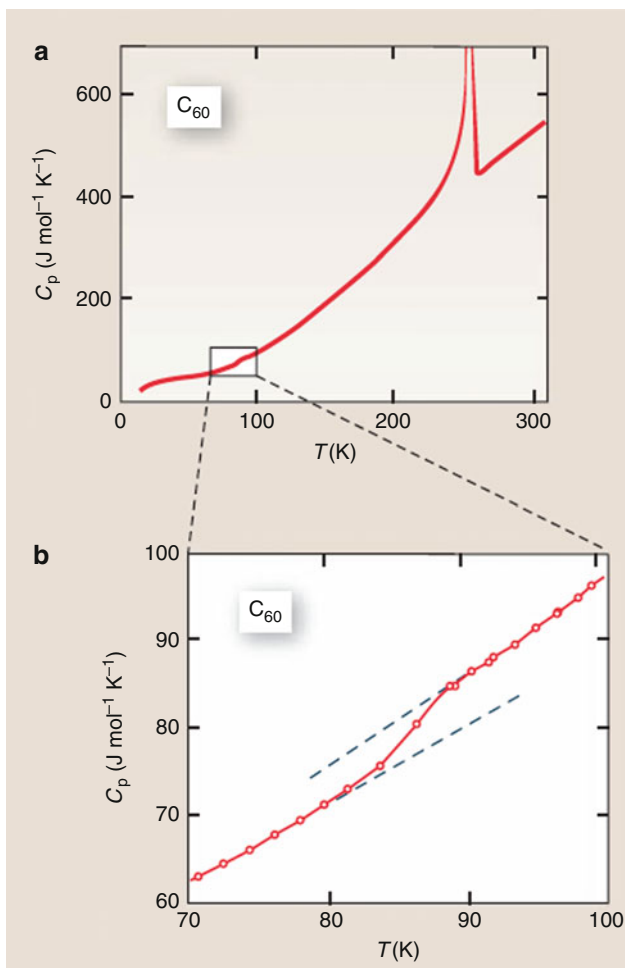


Fig. 2.4 (a) Heat capacity of C_{60} between 0 and 300 K showing order–disorder transition at 260 K (b) Blowup of the small anomaly near 90 K showing a ΔC_p of ≈ 6 J/mol K (From Ref. [4] with permission of AAAS)

The effect of rotational disorder freezing at $t = 1,000$ s, is again extremely weak, but nevertheless has been precisely determined by the adiabatic calorimetry of the Osaka laboratory [17], and its relaxation time could be determined, and shown in accord with the dielectric data [17]. The interesting point here is that the heat capacity function proceeds to a sharp peak at a temperature *almost three times* T_g .

There are many other sharply peaked disordering transitions that have almost no disorder left when they finally undergo a configurational arrest. A good example to compare with the rotational disordering of the substances in Fig. 2.2 is that of NaNO_3 which again has the classical lambda form but no low temperature arrest that can be observed with standard calorimetry. On the other hand, in the case of TiNO_2 for which relaxation time data are seen in Fig. 2.3a, the arrest can be detected and has been described by Moriya et al. [18]. In this case there is no melting phenomenon as in Fig. 2.3b until much higher temperature, and the heat capacity function can be seen to develop into a lambda peak like that of C_{60} .

These systems are clearly characterized by energy landscapes that are rather different in character from those discussed in the literature of glassforming substances [19]. While high states of configurational excitation can obviously be obtained, the states excited are apparently not characterized by energy minima that are separated from neighboring minima by significant energy barriers, by means of which the system can be trapped when the temperature is lowered. Such states are more closely related to anharmonic excitations than to true microstates in the sense that they are usually discussed. Later we will consider the case of a lambda transition in a metallic alloy superlattice that is rather different in character and will be quite useful to our broadened discussion.

Finally there are the intermediate cases where the disordering elements are arranged, center-of-mass-wise, on a crystal lattice like the above cases but can undergo a rotational disordering excitations that have larger volume requirements than the above and are accompanied by much larger heat capacity steps, when the disorder becomes frozen, than the ones discussed above. There seems to be a continuous series here in which the increasing heat capacity jump is accompanied by an increasing departure from Arrhenius behavior of the relaxation. A collection of data taken from the extensive study Brand et al. [20] – to which cases have been added at either extreme by us [21], is shown in Fig. 2.5. This pattern is very similar to that known for the glassforming liquids, but is richer in “strong” glassformer cases. Understanding the manner in which systems make the transition from the lambda type to the typical glassformer type is one of the major statistical thermodynamic problems in this field.

2.2 Glassforming Liquids, Strong and Fragile

With this background we now show the contrasting behavior of different members of the conventional type of glassformer, viz., liquids that slow down with decreasing temperature until they vitrify at T_g , as in Fig. 2.1. To make the immediate contrast with

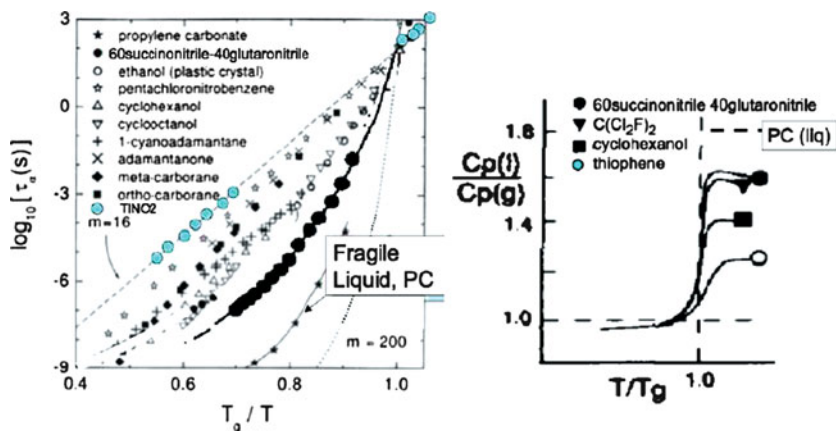


Fig. 2.5 Plastic crystal properties. *Left:* T_g -scaled Arrhenius plot for the relaxation times (mostly dielectric); *right:* T_g -scaled temperature dependence of the heat capacity, relative to that of the glassy state at T_g . (From Ref. [21] by permission) note the correlation of ΔC_p with the position in the scaled Arrhenius plot

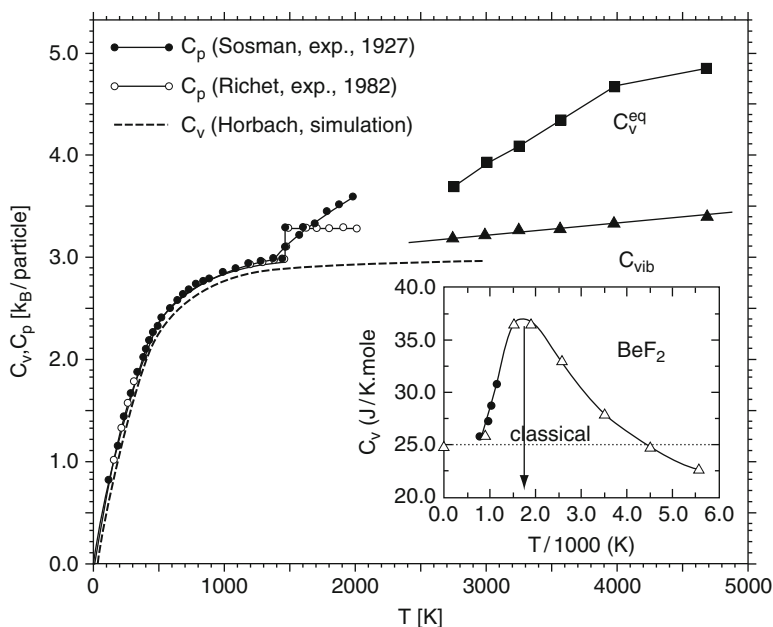


Fig. 2.6 Heat capacity of SiO_2 from experiment (points below 2,000 K) and simulation (points above 2,500 K). The latter are conducted at constant volume which will depress the value below its constant pressure value. A point at 6,100 K that establishes a peak in C_p (Like that seen in the inset for BeF_2) was omitted from this figure in ref. [23]. A peak value for SiO_2 was also evident in earlier studies, by Soules. *Inset:* heat capacity of BeF_2 by experiment (low T points) and simulation (From Ref. [4] by permission)

Fig. 2.1 we show in Fig. 2.6, the available data, experimental [22] and computer simulation [23], for the classical case, SiO_2 . Because of its high glass temperature, the experimental data are limited in range, but they are well supplemented by the computer simulation data on the BKS model of silica [24] that reproduces many silica properties faithfully [25]. The striking difference from the case of the molecular liquid of Fig. 2.1 is reinforced by the data on the weak field analog of SiO_2 , BeF_2 , for which data far above the glass temperature, to $2T_g$, are available [26]. The small jump in C_p for laboratory SiO_2 that was reported in the studies of Ref. [22] almost certainly owes its strength to the presence of some residual OH in the structure, as high temperature DSC studies of truly dry SiO_2 [27] detect essentially no “jump” signal at T_g , despite their superior sensitivity over the drop calorimetry method [22]. This is the implication of the simulation data of Fig. 2.6, when extrapolated back to 1473 K where the viscosity reaches 10^{12} Pa.s, commonly associated with T_g in inorganic glasses. The striking aspect of Fig. 2.6 is not so much the small value of the excess C_p of liquid over crystal at T_g , but the fact that the excess (often called “configurational”) component of the heat capacity rises with increasing temperature, and then peaks at a temperature far above both T_g and T_m . More extensive, but so far unpublished, simulations on BeF_2 (P. H. Poole, private communication) confirm the peak value seen in Fig. 2.6 (insert) [28], and also verify the link-up with the experimental values. Strong liquids apparently behave more like the crystalline materials that exhibit lambda transitions, than they behave like the normal fragile liquids.

We will come back to this similarity a little later but first, for the purposes of this chapter, we need to examine the other extreme in a little more detail. Note in Fig. 2.1 how the difference between liquid and crystal heat capacities is increasing as the temperature decreases. It has been noted by a number of workers [29, 30] that this excess C_p can be well described by a hyperbolic function of temperature, $\Delta C_p = k/T$. Indeed, it is this form of temperature dependence that allows the transformation of the Adam-Gibbs equation for the relaxation time, into the familiar Vogel–Fulcher–Tammann equation [31]. Modeling this form of excess heat capacity has proven rather difficult. The fact that it shows no maximum eliminates the possibility of accounting for the excess with any simple two-state model, as adequately demonstrated on many occasions but particularly by Moynihan and the author [10]. One recent and provocative attempt that *does* account quantitatively for both the excess heat capacity and the excess entropy with the same parameter set, is that of Matyushov and the author [32] whose “Gaussian excitations” model fitting of the data is shown in Fig. 2.7. What is provocative is that the equations that fit the data so well insist that, at a temperature some 10–20% below T_g , the system in equilibrium would undergo a first order transition to a low entropy state, thereby resolving the Kauzmann paradox in an unconventional way.

Before looking further into this matter, we will look at the excess entropy functions seen in Fig. 2.7, in a different way, so as to compare them with the corresponding liquid relaxation time behavior. We plot them in such a way that they have a common value, unity, at the glass transition temperature. This requires a scaling by the value each liquid possesses at T_g .

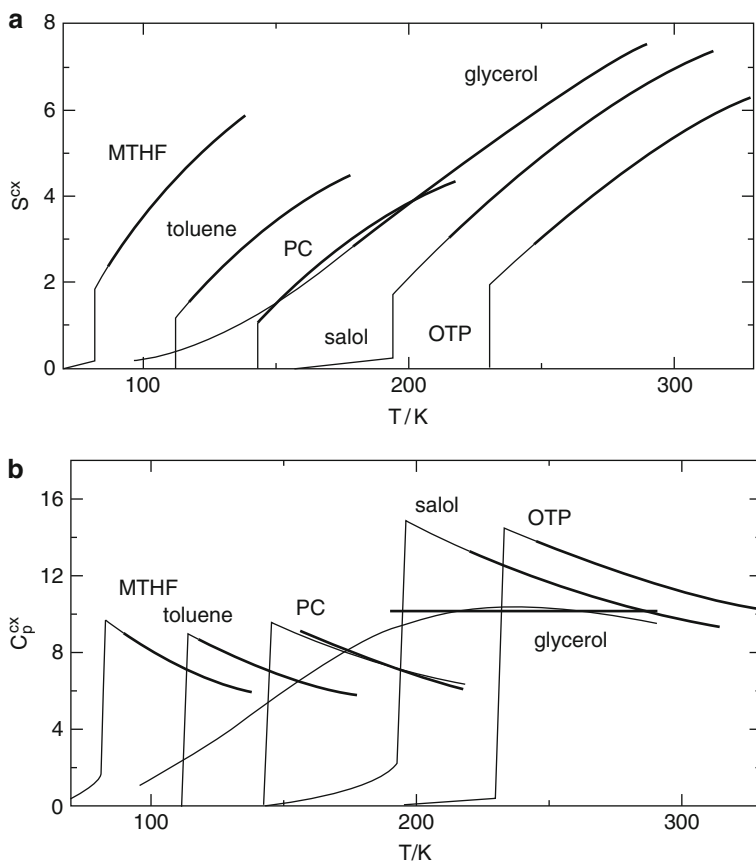
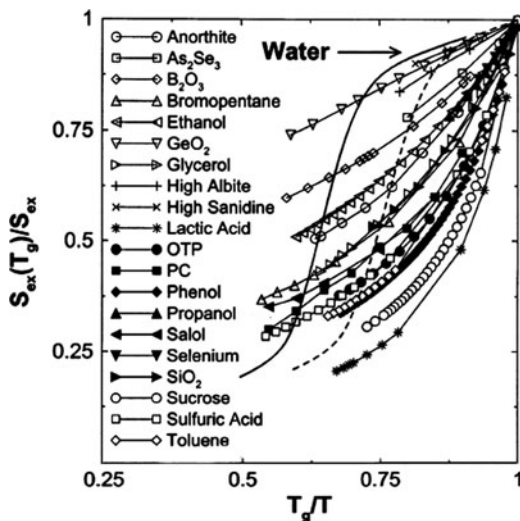


Fig. 2.7 The excess entropy (part (a)) and excess heat capacity part (b) of a series of fragile liquids ($m > 85$). The thick lines are the experimental data and the thin lines are the theoretical best fits continued to lower temperatures to show the predicted first order phase transitions. Only the intermediate liquid, glycerol, the excess heat capacity of which changes little with temperature, offers different behavior. The hyperbolic relation predicts extreme behavior will emerge as liquids of increasingly low cohesion are studied from Ref. [32] by permission

The value of the excess entropy relative to its value at T_g , is presented as a function of inverse absolute temperature scaled by T_g itself, in order that the plot of excess entropies can have the same relation to temperature as does the viscosity in the so-called fragility plot (sometimes given the author's name). This plot, an example of which appears in Fig. 2.5 for plastic crystals, is now used to compare different rates of excitation of the disorder in liquids. Figure 2.8 shows that, as T rises above T_g , some liquids approach the tops of their energy landscapes more rapidly than others. At the top of the landscape, ToL, the entropy per rearrangeable unit $k_B \ln W$ reaches k_B , because all of the e^N microstates are accessible and accordingly $\ln W = 1$. Thus this plot displays the "thermodynamic fragilities", of the liquids in a way that the jump in heat capacity does not. And the thermodynamic

Fig. 2.8 Thermodynamic fragility plot showing the relative rates of excitations of the excess entropy. The case of water is anomalous and implies a lambda like peak in the heat capacity to rationalize the high and low temperature branches of the relative entropy behavior. Reproduced from Angell, C. A. Chem. Rev. 102,2627 (2002) by permission



fragilities correlate with the kinetic fragilities [33] in a manner that the jump in heat capacity does not [34]. The scaling by the excess entropy at T_g makes the display independent of the choice of number of “beads” [32, 35–37] per mole of liquid, but does not safeguard against anomalous entropies of fusion due to anomalously high entropies in the crystalline state, and the latter will invalidate the assumption that the crystalline state entropy represents the vibrational entropy of the liquid at its melting point. Thus the position of SiO_2 in this plot is anomalous, unless the excess entropy is assessed by thermodynamic integration from the ideal gas state, and subtraction of a harmonic entropy, as was done in Ref. [38].

There is one liquid in this plot that behaves in a highly anomalous manner. That liquid is water, about which much is known but much also remains mysterious. Water, which can be vitrified by a number of alternative routes, is known to have an extremely weak glass transition, but it also has, according to two independent assessments [39, 40] a very small entropy at its T_g . Thus at the extreme of high temperature its relative entropy is expected to be large. At the same time, its extremely weak calorimetric glass transition, comparable to that seen in Fig. 2.3 for dipole disordering in C_{60} , means that the rate of excitation of entropy immediately above T_g is very small. Thus, it appears like the strongest liquid near T_g , but higher in temperature, in the moderately supercooled liquid region where its entropy relative to ice is well known, its excess entropy is very high. Accordingly, in the intermediate range where direct observations cannot be made because of the instability of the liquid against crystallization (hence the description “no-man’s land”), the excess entropy must undergo a very rapid change. This entropy would be associated with a hidden lambda transition, or to a hidden first order transition like that seen in supercooled silicon in the Stillinger–Weber model [41], and more

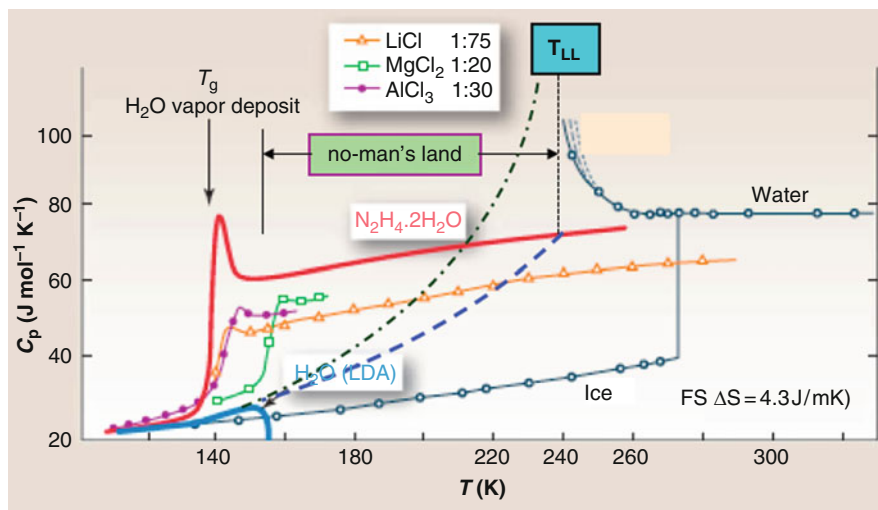


Fig. 2.9 Heat capacity of water in normal, supercooled liquid and glassy states, showing two possible interpolations to preserve a continuity that must exist in view of the vitrifiability of liquids water under sufficiently high cooling rates (From Ref. [4] by permission of AAAS)

recently in *ab initio* simulations. These two options are shown in Fig. 2.9 and are seen to make a very plausible rationalization of the observations made in the two accessible regions (near the melting point on the one hand and near T_g on the other).

Figure 2.8 contains only experimental data except for the case of water where there is a data gap between high and low T (discussed below). The presence of peaks in the high temperature heat capacity of BeF_2 , and to a lesser extent SiO_2 from simulation studies (Fig. 2.6), suggests that these (and perhaps other strong liquids as well), might show water-like behavior at higher temperatures when the extended measurements (particularly at higher pressures) become available.

Water and its anomalies are often discussed in terms of the presence of a second critical point that occurs just beyond the range of observability [42–45]. Opinions differ on whether it lies at positive or negative pressures [4], with some suggesting it might even be subsumed into the liquid–gas spinodal as suggested by the stability limit conjecture of Speedy [46] (in updated form to include a second spinodal for the low density liquid). Such a “critical point-free” scenario [4] is after all, the form that is suggested by all the empirical equations of state for water [47], though these seem to be generally discounted by workers in the field. On the other hand, if the second critical point not only exists but also were, serendipitously, to fall at ambient pressure, then the heat capacity curve for *ambient pressure* water would (in absence of crystallization) have *exactly* the lambda form, since a critical point transition is one example of this very general cooperative transition. This is indicated as the upper (dash-dotted) curve in Fig. 2.9. The lower dashed curve corresponds to the case of a weak first order transition that would occur at ambient pressure if the critical point lies at negative pressure or is subsumed into the liquid–spinodal.

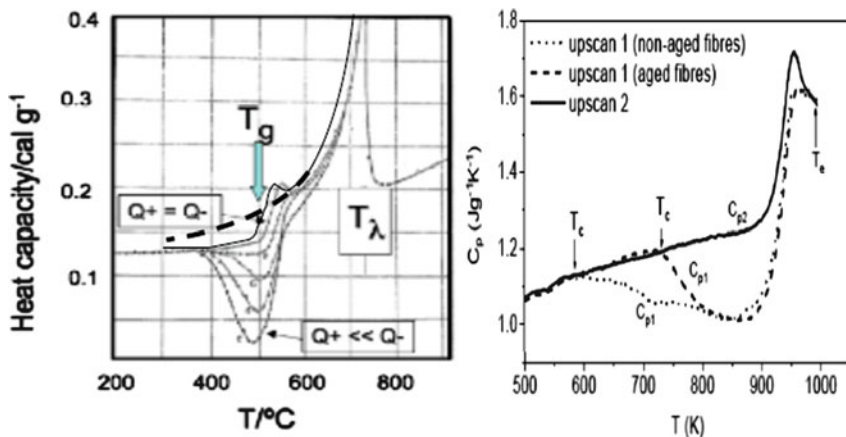


Fig. 2.10 Comparison of the apparent heat capacity responses of CoFe alloy and a silicate glass after comparable thermal treatments. The darkest curves, in each case, are the standard glass transitions obtained when heating and cooling rates are the same. The lowermost curves are when the cooling rates were the most different (very fast in each case, corresponding to quenching in the most disorder. In each case the most disordered structure is the one trapped in a basin of smallest depth, but the difference in temperature between the standard T_g and the temperature where the quenched system starts when the real glass starts to relax, is much greater in the case of real glass. Notably, glassy water exhibits behavior closer to that of the alloy, where the thermal relaxation peak for the quenched state, has a sharper peak starting at T closer to T_g (From Ref. [48, 49] respectively, with the author's permission)

To complete our development of this increasingly broad picture of the glass transition under development in this chapter, it is important to add one further, and very informative, example of the lambda transition. This is the transition that occurs in the alloy superlattice, $\text{Co}_{50}\text{Fe}_{50}$. It is needed in order to make clear that, when the elementary step of the excitation process in a lambda type order–disorder transition is one which involves barrier crossing with substantial activation energy, this type of thermodynamic transition can support an ergodicity-breaking that has all the rate-dependent phenomena of the usual glass transition.

The heat capacity of this system was studied by Kaya and Sato [48], using different, increasingly severe, quenching procedures that arrested the ordering process in different states of excess entropy. The behavior of these were then evaluated during reheating at a fixed rate for comparison with the behavior observed when the cooling rate was the same as the standard heating rate (the darkened curve in Fig. 2.10). In Fig. 2.10 the observations are displayed alongside the more recent study of Yue and Jensen [49] for a silicate glass subject to a similar procedure (namely quenching very rapidly from well above T_g followed by reheating at the standard rate of 20 K/min) that has qualitatively similar consequences (see also [50]). The darker curve is, in each case, for the condition, *cooling rate* = *subsequent heating rate*. In the case of Fig. 2.10a, the dashed line recalls what we know would happen if no ergodicity-breaking were to occur, since (unlike the glass transition equilibrium heat capacity) we know the lambda heat capacity form.

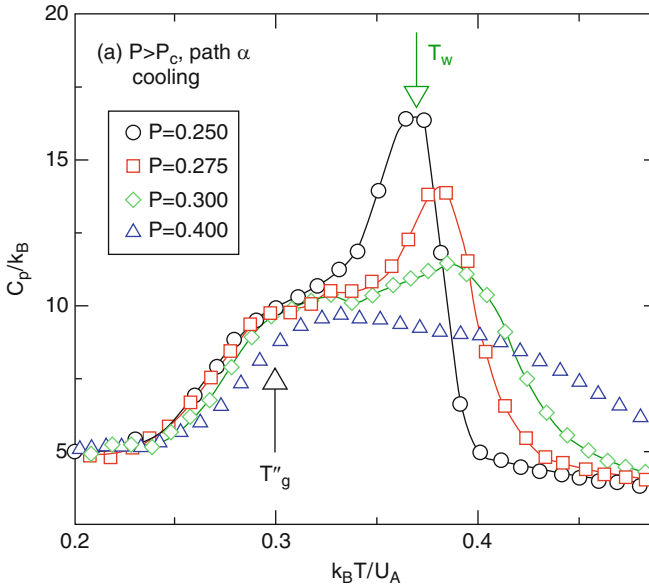


Fig. 2.11 The constant pressure liquid heat capacity of the attractive Jagla model, for isobars of pressure close to, and increasingly above, the critical pressure of 0.235, showing the peak in heat capacity associated with super-critical fluctuations, which diminish with increasing distance from the critical point. The peak temperatures define the so-called Widom line. note that the cooling glass transition are always below the peak temperature (From Ref. [51], by permission of the American Physical Society)

With this background on ergodicity-breaking in a system with a lambda transition, let us now return to what happens when the conditions in a liquid system with a critical point are changed so that the critical point is narrowly missed and only the supercritical fluctuations are encountered. The behavior may be seen in the results of a recent study by Xu et al. [51] extended by Buldyrev et al. [52], of a model system that has been parameterized to have a liquid–liquid transition in the stable liquid domain [53]. This is the ramp model of Jagla [54] with attractive component of the potential included. The temperature dependence of the isobaric heat capacity for this system, at a series of pressures increasing in value above the critical pressure, is shown in Fig. 2.11. The point to be emphasized here is the increasingly rounded forms as the isobars cross the extension of the coexistence line beyond the critical point (now becoming known as the Widom line). The strength of the transition that “gathers-in” the peak of the cooperative transition at T_c is seen to dissipate to higher temperatures as the isobar departs increasingly from the critical point. Sufficiently far from T_c the effect of critical point vanishes and one is left with something reminiscent of the metallic glassformer heat capacity. The similarity of the lowest pressure isobar (the $p = 0.240$ “scan”) to the heat capacity behavior of the Co–Fe alloy (Fig. 2.10 left) when heating and cooling rates are the same, can hardly be missed.

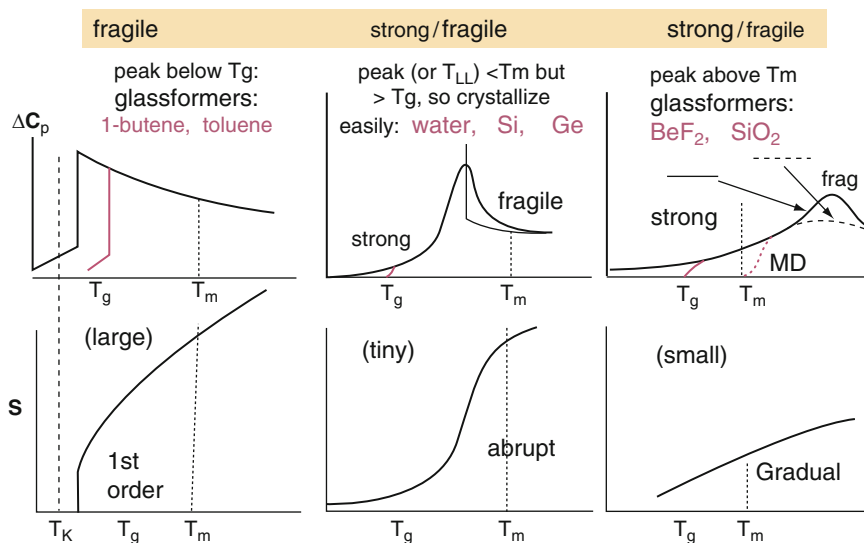


Fig. 2.12 Changeover in the forms of excess heat capacity, and excess entropy, above the glass transition on passing from “strong” inorganic network glasses to “fragile” molecular glasses. Strong network liquids appear like expanded order–disorder transitions (see final section) and when pure may have tiny glass transitions, while fragile molecular liquids have large ΔC_p glass transitions and their ordering limits are depressed below T_g . Water, a tetrahedral network based on hydrogen bonding, lies at the crossover between the two classes of behavior. This can be interpreted in terms of the increasing Gaussian width in the distribution of excitation energies, and consequent increasing disorder stabilization of the excitations. This implies that the ordering in liquids during temperature decrease is an increasingly cooperative de-excitation process when changing from network to molecular liquid glassformers (From Ref. [2] by permission of Materials Research Society)

With these examples in mind we can then present the series of heat capacity and entropy functions that we have recently included in articles that attempt to describe a broader view of the glass transition phenomenon [2, 55]. The pattern of heat capacities has been viewed in terms of the effects of increasing cooperativity in the excitation process as we pass from strong network glasses, at one extreme, through the intermediate strength network represented by water, to non-network liquids like the preponderance of glassformers of common experience, ending in the very fragile liquids in which only the high temperature side of the transition is seen, because the low temperature side is hidden by the glass transition. Actually, most of the low temperature side of the transition in these cases, according to theory [32], is cut off by first order transitions to a de-excited low entropy state. Being, in most cases, a structure that is closer to that of the crystal form, than the viscous liquid from which it formed, this low enthalpy phase can often serve as a stepping stone to the crystalline state (the Ostwald rule of stages, in action). The rapid crystallization of second liquid phases, when they form above the glass transition, [56, 57] is one of the factors that has made the study of these phenomena confusing.

It is striking that the two cases, water and silicon, in which the presence of a continuous or weak first order transition has been most clearly seen, are two of the poorest glassformers known [55] (at least when high pressure quenchings are excluded [58]), this being a consequence of the fact that the transition, with its large entropy fluctuations generates copious nuclei of the stable crystalline phase which can only be avoided by hyperquenching, vapor deposition, or pressure-induced amorphization. Via the pressure path, large samples of both amorphous phases have now been grown [59].

There are two very important linked implications of Fig. 2.12 to emphasize here. The first concerns the heat capacity function on the right hand side of the figure (with its peak only at very high temperatures). This makes us realize that the behavior observed in the laboratory for *strong* liquids is the behavior of systems exploring the low temperature side of an order–disorder transition that has been smeared out as in Fig. 2.11, by being off-critical to a true lambda transition that in principle could be experienced at a liquid–liquid critical point at higher pressures. Thus the system studied in the laboratory is sensing only the approach to a maximum in fluctuations at the Widom line.

The second is the linked implication that, just as the correlation length for fluctuations increases as a critical point in a single phase system (e.g. $\text{Co}_{50}\text{Fe}_{50}$ of Fig. 2.10a, or the lambda transition in C_{60}) is approached from below, so must the correlation length for fluctuations increase with increasing temperature in the range explored by the laboratory strong liquids. This is of particular interest in the case of silica where the fluctuations, via their Fourier components, will affect the scattering of light because the scattering of light is of central concern in the optical fibers used for information transfer (not to mention the silica glass lasers used in laser fusion technology). Indeed, the evidence from light scattering studies conducted in relation to fiber fictive temperature, confirms our expectations [60].

The importance of this is that it is just the opposite temperature dependence of correlation length to that supposed by glass theorists who, it must be recognized, have always been concerned with fragile liquids. The theorists, however, have tended to adopt the increasing correlation length idea as a fundamental interpretation of viscous slow-down, hence of glass formation, and the fact that the relation between correlation length and relaxation time is inverted when it comes to the classical silicate glasses (and other strong liquids, presumably) is a warning that the universality aspects of the glass transition must be sought elsewhere. For strong liquids it can now be appreciated that any effect of correlation length on the dynamics will be in opposition to that of any natural barrier- crossing kinetics that exist, hence will oppose the slowdown, while for fragile liquids it will enhance the slowdown. Whether this can be considered as an explanation of the difference between strong and fragile liquid kinetics is a little difficult to say. We note, however, that in lambda transitions, the simple Arrhenius form of kinetics is followed over many orders of magnitude (e.g. TiNO_2 [18] in Fig. 2.3a, and C_{60} [61]) while the magnitude of the fluctuations increases and the correlation length accordingly starts to diverge.

The presence of first order transitions below T_g , predicted by the analysis of Ref. [32] would be consistent with the current findings of ultrastable [62], and ultradense [63], glasses formed by vapor deposition processes on controlled temperature substrates, when the temperature is controlled at some 10–20% below the standard T_g . These are reported [64] to convert back to viscous liquids via nucleation and growth processes – the hallmark of a first order transition. The one micron length scale reported for the process [64] is reminiscent of the homogeneous nucleation of ice crystals from aqueous LiCl solutions near T_g [65], now known to be consequent on the prior polyamorphous transformation of vitreous water [66]. Whether these new phases are truly amorphous or are some higher order disordered crystal form transitional to the ground state crystal (hence another example of the Ostwald rule of stages in action) has yet to be definitively decided. A true first order character would be expected if the liquid–liquid transition implicit in the behavior of SiO_2 at high pressure becomes modified to occur near ambient pressure for the weaker network H_2O and then passes to negative pressure domain for the more weakly interacting but more cooperative van der Waals liquids. It will require much more work to establish whether or not such a simple set of systematic changes across such a broad swath of liquids, can be supported.

Irrespective of the outcome on the latter question, it should be clear from the material of this chapter that a rich panoply of thermodynamic behavior accompanies the transition of non-ergodic to ergodic states of condensed matter, in particular the case of glassy solid to non-viscous liquid, and that much systematic work remains to be done before the complex patterns of behavior can be fully understood.

Acknowledgments Support of the NSF, DMR (Solid State Chemistry) and Chemistry divisions, Grant numbers 0454672 and 0404714, is gratefully acknowledged. We have profited from helpful discussions with Dmitry Matyushov and Ranko Richert. Yuanzheng Yue, Thomas Loerting and group, Masaharu Oguni Gene Stanley Sergey Buldyrev and group, Srikanth Sastry, Pablo Debenedetti and Mark Ediger.

References

1. Debenedetti PG (1976) *Metastable liquids: concepts and principles*. Princeton University Press, Princeton, NJ
2. Angell CA (2008) Glassformers and viscous liquid slowdown since David Turnbull: enduring puzzles and new twists (text of Turnbull lecture). *MRS Bull* 33:545–555
3. Takeda K, Yamamuro O, Oguni M, Suga H (1995) Calorimetric study on structural relaxation of 1-pentene in vapor-deposited and liquid-quenched glassy states. *J Phys Chem* 99:1602–1607
4. Angell CA (2008) Insights into phases of liquid water from study of its unusual glass-forming properties. *Science* 319:582–587
5. Debenedetti PG, Stillinger FH (2001) Supercooled liquids and the glass transition. *Nature* 410:259–267
6. Angell CA (1995) Formation of glasses from liquids and biopolymers. *Science* 267:1924–1935

7. Cohen MH, Turnbull D (1959) Molecular transport in liquids and glasses. *J Chem Phys* 31:1164–1169
8. Adam G, Gibbs JH (1965) On temperature dependence of cooperative relaxation properties in glass-forming liquids. *J Chem Phys* 43:139–146
9. Dyre JC, Olsen NB, Christensen T (1996) Local expansion model for viscous-flow activation energies of glassforming molecular liquids. *Phys Rev B* 53:2171–2174
10. Moynihan CT, Angell CA (2000) Bond lattice or excitation model analysis of the configurational entropy of molecular liquids. *J Non-Cryst Solids* 274:131–138
11. Angell CA, Rao KJ (1972) Configurational excitations in condensed matter and the bond lattice model for the liquid-glass transition. *J Chem Phys* 57:470–481
12. Saika-Voivod I, Sciortino F, Poole PH (2004). Free energy and configurational entropy of liquid silica: fragile-to-strong crossover and polyamorphism. *Phys Rev E* 69:041503(13)
13. Faupel F, Frank W, Macht MP, Mehrer H, Naundorf V, Ratzke K, Schober HR, Sharma SK, Teichler H (2003) Diffusion in metallic glasses and supercooled melts. *Rev Mod Phys* 75:237–280
14. Fujimori H, Oguni M (1995) Correlation index (T_g-T_{gb})/T_g and activation energy ratio as parameters characterising the structure of liquid and glass. *Solid State Commun* 94:157–162
15. Fujimori H, Oguni M (1993) Construction of an adiabatic calorimeter at low temperatures and the glass transition of crystalline 2-bromothiophene. *J Phys Chem Solids* 54:271–280
16. Fujita H, Fujimori HO, Oguni M (1995) Glass transitions in the stable crystalline state of dibenzofuran and fluorene. *J Chem Thermodyn* 27:927–938
17. Matsuo T, Suga H, David WIF, Ibberson RM, Bernier P, Zahab A, Fabre C, Rassat A, Dworkin A (1992) The heat-capacity of solid C-60. *Solid State Commun* 83:711–715
18. Moriya K, Matsuo T, Suga H (1983) Phase transitions and freezing of ion disorder in CsNO₂ and TiNO₂ crystals. *J Phys Chem Solids* 44:1103–1119
19. Wales DJ (2003) Energy landscapes, Cambridge molecular science series. Cambridge University Press, Cambridge
20. Brand R, Loidl A, Lunkenheimer P (2002) Relaxation dynamics in plastic crystals. *J Chem Phys* 116:10386–10401
21. Mizuno F, Belieres J-P, Kuwata N, Pradel A, Ribes M, Angell CA (2006) Highly decoupled ionic and protonic solid electrolyte systems, in relation to other relaxing systems and their energy landscapes. *J Non-Cryst Solids* 352:5147–5155
22. Richet P, Bottinga YD, Denielou L, Petitiet JP, Tegui C (1982) Thermodynamic properties of quartz, cristobalite and amorphous SiO₂: drop calorimetry measurements between 1000 and 1800 K and a review from 0 to 2000 K. *Geochim Cosmochim Acta* 46:2639
23. Scheidler P, Kob W, Latz A, Horbach J, Binder K (2005) Frequency-dependent specific heat of viscous silica. *Phys Rev B* 63:104204(14)
24. van Beest BWH, Kramer GJ, van Santen RA (1990) Force fields for silicas and aluminophosphates based on *ab initio* calculations. *Phys Rev Lett* 64:1955–1958
25. Vollmayr K, Kob W (1996) Investigating the cooling rate dependence of amorphous silica: a computer simulation study. *Ber. bunsenges. Phys Chem* 100:1399–1401
26. Tamura S, Yokokawa T, Niwa K (1975) The enthalpy of beryllium fluoride from 456 to 1083 K by transposed-temperature drop calorimetry. *J Chem Thermodyn* 7:633
27. Videa M, Angell CA (unpublished work)
28. Hemmati M, Moynihan CT, Angell CA (2001) Interpretation of the molten BeF₂ viscosity anomaly in terms of a high temperature density maximum, and other waterlike features. *J Chem Phys* 115:6663–6671
29. Privalko Y (1980) Excess entropies and related quantities in glass-forming liquids. *J Phys Chem* 84:3307–3312
30. Alba C, Busse LE, List DJ, Angell CA (1990) Thermodynamic aspects of the vitrification of toluene, and xylene isomers, and the fragility of liquid hydrocarbons. *J Chem Phys* 92:617–624

31. Angell CA, Bressel RD (1972) Fluidity and conductance in aqueous electrolyte solutions. An approach from the high concentration limit. I. $\text{Ca}(\text{NO}_3)_2$ solutions. *J Phys Chem* 76:3244–3252
32. Matyushov D, Angell CA (2007) Gaussian excitations model for glassformer thermodynamics and dynamics. *J Chem Phys* 126:094501(19)
33. Martinez L-M, Angell CA (2001) A thermodynamic connection to the fragility of glass-forming liquids. *Nature* 410:663–667
34. Huang D-H, McKenna GB (2001) New insights into the fragility dilemma in liquids. *J Chem Phys* 114:5621–5630
35. Wunderlich B (1960) Study of the change in specific heat of monomeric and polymeric glasses during the glass transition. *J Phys Chem* 64:1052–1056
36. Moynihan CT, Angell CA (2000) Bond lattice or excitation model analysis of the configurational entropy of molecular liquids. *J Non-Cryst Solids* 274:131–138
37. Stevenson JD, Wolynes PG (2005) Thermodynamic-kinetic correlations in supercooled liquids: critical survey of experimental data and predictions of the random first order transition theory of glasses. *J Phys Chem B* 109:15093–15097
38. Saika-Voivod I, Poole PH, Sciortino F (2001) Fragile-to-strong transition and polyamorphism in the energy landscape of liquid silica. *Nature* 412:514–517
39. Whalley E, Klug DD, Handa YP (1989) Entropy of amorphous ice. *Nature* 342:782–783
40. Speedy RJ, Debenedetti PG, Smith RS, Huang C, Kay BD (1996) The evaporation rate, free energy, and entropy of amorphous water at 150 K. *J Chem Phys* 105:240–244
41. Sastry S, Angell CA (2003) Liquid–liquid phase transition in supercooled liquid silicon. *Nat Mater* 2:739–743
42. Poole PH, Sciortino F, Essmann U, Stanley HE (1992) Phase-behavior of metastable water. *Nature* 360:324–328
43. Tanaka H (2002) Simple view of water-like anomalies of atomic liquids with directional bonding. *Phys Rev B* 66:064202(8)
44. Brovchenko I, Geiger A, Oleinikova A (2005) Liquid–liquid phase transitions in supercooled water studied by computer simulations of various water models. *J Chem Phys* 123:044515(16)
45. Poole PH, Sciortino F, Grande T, Stanley HE, Angell CA (1994) Effect of hydrogen bonds on the thermodynamic behavior of liquid water. *Phys Rev Lett* 73:1632–1635
46. Speedy RJ (1982) Stability-limit conjecture. *J Phys Chem* 86:982–989
47. Wagner W, Pruss A (2002) The IWAPS formulation 1995 for the thermodynamic properties of ordinary water substance for general and scientific use. *J Phys Chem Ref Data* 31:387–535
48. Kaya S, Sato H (1943) Superstructuring in the iron–cobalt system and their magnetic properties. *Proc Physico-Math Soc Japan* 25:261–273
49. Yue YZ (2004) Influence of physical ageing on the excessive heat capacity of hyperquenched silicate glass fibres. *J Non-Cryst Solids* 348:72–77
50. Angell CA, Yuanzheng Y, Wang L, Copley JRD, Borick S, Mossa S (2003) *J Phys cond Matt* 15: S1051–S1068
51. Xu L-M, Buldyrev SV, Giovambattista N, Angell CA, Stanley HE (2009) A monatomic system with a liquid–liquid critical point and two glassy states. *J Chem Phys* 130:054505(12)
52. Buldyrev SV, Malesio G, Angell CA, Giovambattista N, Prestipino S, Saija F, Stanley HE, Xu L (2009) Unusual phase behavior of one-component systems with two-scale isotropic interactions. *J Phys Condens Mat* 21:504106(18)
53. Xu L, Buldyrev SV, Angell CA, Stanley HE (2006) Thermodynamics and dynamics of the two-scale spherically-symmetric Jagla model of anomalous liquids. *Phys Rev E* 74:031108(10)
54. Jagla EA (1998) Phase behavior of a system of particles with core collapse. *Phys Rev E* 58:1478–1486
55. Angell CA (2008) Glass formation and glass transition in supercooled liquids, with insights from study of related phenomena in crystals. *J Non-Cryst Solids* 354:4703–4712

56. Mizukami M, Kobashi K, Hanaya M, Oguni M (1999) Presence of two freezing-in processes concerning a-glass transition in the new liquid phase of tri-phenylphosphite. *J Phys Chem B* 103:4078–4088
57. Aasland S, Mcmillan PF (1994) Density-driven liquid–liquid phase-separation in the system $\text{Al}_2\text{O}_3\text{--Y}_2\text{O}_3$. *Nature* 369:633–636
58. Bhat H, Molinero V, Soignard E, Solomon VC, Sastry S, Yarger JL, Angell CA (2007) Vitrification of a monatomic metallic liquid. *Nature* 448:787–790
59. Loerting T, Winkel K, Kohl I (submitted for publication: private communication) 2010
60. Sakaguchi S, Todoroki S-I (1998) Rayleigh scattering of silica core optical fiber after heat treatment. *Appl Opt* 37:7708–7711
61. Mondal P, Lunkenheimer P, Boehmer R, Loidl A, Gugenberger F, Adelmann P, Meingast C (1994) Dielectric relaxation dynamics in C-60 and C-70. *J Non-Cryst Solids* 172:468–471
62. Swallen SF, Kearns KL, Mapes MK, Kim YS, McMahon RJ, Wu T, Yu L, Ediger MD (2007) Organic glasses with exceptional thermodynamic stability and kinetic stability. *Science* 315:354–356
63. Ishii K, Nakayama H, Hirabayashi S, Moriyama R (2008) Anomalously high-density glass of ethylbenzene prepared by vapor deposition at temperatures close to the glass-transition temperature. *Chem Phys Lett* 459:109–112
64. Kearns KL, Ediger MD, Huth H, Schick C (2010) One micrometer length scale controls kinetic stability of low energy glasses. *J Phys Chem Lett* 1:388–392
65. Dupuy J, Chieux P, Calemzuk R, Jal JF, Ferradou C, Wright A, Angell CA (1982) Controlled nucleation and quasi-ordered growth of ice crystals from low temperature electrolyte solutions: a small angle neutron scattering study. *Nature* 296:138–140
66. Mishima O (2007) Phase separation in dilute $\text{LiCl--H}_2\text{O}$ solution related to the polyamorphism of liquid water. *J Chem Phys* 126:244507(5)

Glassy, Amorphous and Nano-Crystalline Materials
Thermal Physics, Analysis, Structure and Properties

Šesták, J.; Mareš, J.J.; Hubík, P. (Eds.)

2011, XVII, 380 p., Hardcover

ISBN: 978-90-481-2881-5